Thermochimica Acta, 122 (1987) 197–207
Elsevier Science Publishers B.V., Amsterdam — Printed in The Netherlands

CONTRIBUTION OF MICROCALORIMETRY TO THE STUDY OF ADSORPTION MECHANISMS OF IONIC AND NON-IONIC MOLECULES AT THE SOLID-WATER INTERFACE

F. THOMAS [1], J. Y. BOTTERO [1], S. PARTYKA [2], D. COT [2].

1 Centre de Recherche sur la Valorisation des Minerais, UA 235 du CNRS, BP 40, 54500 VANDOEUVRE CEDEX

2 Laboratoire de Physicochimie des Systèmes Polyphasés, UA 330 du CNRS, Université des Sciences et Techniques du Languedoc, Place Eugène Bataillon, 34000 MONTPELLIER.

SUMMARY

Adsorption of an ionic surfactant (Octyl Benzene Sulfonate: OBS), sodium salicylate, and a nonionic surfactant (octylphenyl polyoxyethylene: TX 100) onto hydrophilic (silica and alumina) and hydrophobic (activated carbon) surfaces was studied by batch adsorption microcalorimetry combined with the adsorption isotherms. Comparison between the corresponding enthalpic curves showed: 1. the micellar structure of TX 100 adsorbed on the silica, 2. the liquid crystal state of OBS adsorbed on alumina, 3. the interactions of the alkyl chain of the surfactants and the benzene ring common to the three adsorbates with the activated carbon surface.

INTRODUCTION

The study of adsorption mechanisms at the solid-liquid interface usually implies the use of direct spectroscopic methods such as NMR (1,2), EPR (3), and electrophoretic methods (4,5). Microcalorimetry is one of the most effective methods for the simultaneous measurment of:

- the enthalpy of displacement of adsorbed water molecules by a solute.
- the accompanying conformational modification of the adsorbed molecules.

Among the techniques used, immersion calorimetry has shown the distribution of trains and loops formed by the macromolecules of polyethylene glycol adsorbed from an organic solution on an Aerosil silica (6-8). New stirring systems inside calorimetric cells (9-11) have resulted in greater sensitivity (25 μV full scale) and small variations in the adsorption rate can now be detected (12). The technique has recently been used for the study of the adsorption of polyacrylamide at the Montmorillonite-water interface (2). Conformational changes in the adsorbed phase with increasing surface coverage, as well as the textural evolution of the clay tactoids were demonstrated.

Flow- calorimetry has recently been developed in the field of enhanced oil recovery (13-16) and also provides direct measurements of desorption enthalpies.

The aim of this paper is to illustrate the ability of microcalorimetry in order to study

0040-6031/87/$03.50

the adsorption mechanisms of organic molecules at the solid-water interface. To this effect the adsorption of three adsorbates: a nonionic surfactant (TX 100), an anionic surfactant (OBS Na) and a molecule without alkyl chain (sodium salicylate) on three adsorbents : an alumina and a silica (hydrophilic surface), and an activated carbon (hydrophobic surface) was studied.

MATERIALS

Adsorbents

The three solids: a spherosil silica (XOB 015), an alumina (MERCK 90A) and an activated carbon (CECA 1240) were of high chemical purity. Two types of properties were taken into account:

- The texture was determined from nitrogen adsorption-desorption isotherms at 77°K . The specific surface areas were calculated by the BET method. The size distribution of the mesopores was determined according to the desorption hysteresis by the B.J.H method. The porosity of the activated carbon ranged from 0.5 to 4.5 nm in diameter with a great predominance in micropores lower than 2 nm (17). The alumina was mesoporous with a maximum around 5 nm (18). The silica was not porous. All the values are reported in Table 1.

TABLE 1
Textural Properties of the Adsorbents

	SILICA Spherosil	ACTIVATED CARBON CECA 1240	ALUMINA MERCK 90 A
Specific Surface Area ($m^2.g^{-1}$)	25	1088	107
Porosity (nm)	no porosity	0.5 to 4.5 micropores	3 to 30 mesopores

- The superficial electric properties were determined by means of electrophoresis using a LASER ZEE METER model 501. The superficial sites of hydrophilic mineral adsorbents (silica and alumina) behaved like diprotic acids according to the following equilibria where =S is the surface site :

$$=S\text{-}OH_2^+ \rightleftharpoons =S\text{-}OH + H^+ \qquad (1)$$

$$=SOH \rightleftharpoons =SO^- + H^+ \qquad (2)$$

In low ionic strength medium (KCl 10^{-3} M) their isoelectric points (IEP) were obtained at pH=3.5±0.2 for the silica and at pH=8.5±0.2 for the alumina (Fig.1). The surface was positively charged (eq.1), and negatively charged (eq.2) for pH < IEP and > IEP respectively.

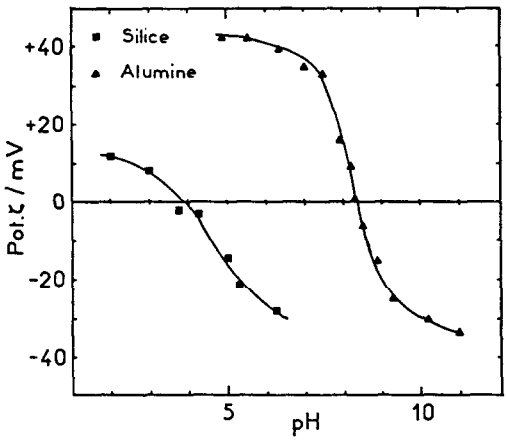

Fig.1. Electrokinetic Potential (ζ Potential) of Silica and Alumina.

Adsorbates

The adsorbates were :

- an anionic surfactant : sodium octylbenzene sulfonate (OBS)

$C_8H_{17}C_6H_4SO_3^-Na^+$

- a nonionic surfactant : octylphenyl polyoxyethylene (TX100)

$C_8H_{17}C_6H_4(O\text{-}CH_2CH_2)_{9\text{-}10}$

- sodium salicylate

$C_6H_4OHCOO^-Na^+$

Their physicochemical properties are reported in Table 2.

TABLE 2

Properties of the Adsorbates.

	TX 100	O B S	SALICYLATE
Molecular Weight	64.6	292.3	160.11
Solubility (mol. l^{-1})	infinite	infinite	0.1
Molecular Area (nm^2)	0.5	0.35	0.205
Turbidity Point (°C)	65	-	-
C. M. C. (mol. l^{-1})	$2.8\ 10^{-4}$	$1.2\ 10^{-2}$	-
KRAFFT Point (°C)	-	18.5	-
pK1	-	1.5	2.7
pK2	-	-	13.9

EXPERIMENTAL

Adsorption isotherms

The adsorption isotherms were obtained by the rest method: an adsorbent mass (m) corresponding to a surface area of about 10 to 100 m^2 was immersed in a volume (V) of 20 ml of an adsorbate solution at known concentration (C_o). Equilibrium was reached after 24 hours with stirring at 35°C. The suspension was then centrifuged and the equilibrium concentration of the supernatant (C_e) was determined by UV spectroscopy (275.5 nm for TX 100, 222 nm for OBS, 296 nm for the salicylate). The adsorbed amount Γ was calculated as follows:

$$\Gamma = (C_o - C_e).\ V / m$$

The pH during the experiments ranged between 6 and 6.5 for the silica, 4.5 to 7.5 for the alumina and 7 to 7.5 for the activated carbon.

Microcalorimetry

The adsorption heat measurements were carried out at 35°C using a CALVET differential microcalorimeter (19). Each cell contained the adsorbent suspension topped by a tank enclosing the reagent (adsorbate solution in the laboratory-cell, water in the reference-cell). Small amounts of reagent were injected into the adsorbent suspension by means of a peristaltic pump. The suspension was continuously stirred by a propellor connected outside with a rod and driven by a rotating magnet (Fig.2). The thermal effects were recorded as a function of time for each injection.

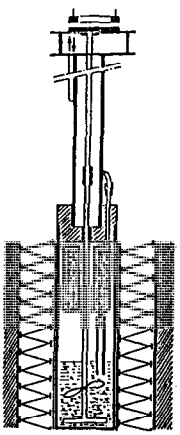

Fig. 2. Experimental Device for Microcalorimetry.

The enthalpy due to the adsorption was calculated by subtracting the molar dilution enthalpy of

the adsorbate from the raw molar enthalpy of the reaction. In reality, this is a displacement enthalpy ($\Delta_{dis}H$) since adsorption of a molecule at the solid-liquid interface ($\Delta_{dis}H$) requires the desorption of several structured water molecules ($\Delta_{dis}H$) , and their replacement by the adsorbate (20). The calorimetric signal sums up these two phenomena according to the following equation:

$$\Delta_{dis}H = \Delta_{ads}H + \Delta_{des}H$$

The molar enthalpy of displacement $\Delta_{dis}h$ is equal to the ratio of the enthalpy of displacement $\Delta_{dep}H$ divided by the number of adsorbed molecules n_a:

$$\Delta_{dis}h = \Delta_{dis}H/n_a$$

RESULTS

Adsorption isotherms

The adsorption isotherms normalized by BET specific surface area show the evolution of the adsorbed quantity Γ in $\mu mol.m^{-2}$) as a function of the residual concentration Ce in $mol.l^{-1}$.

A) TX100 (Fig.3)

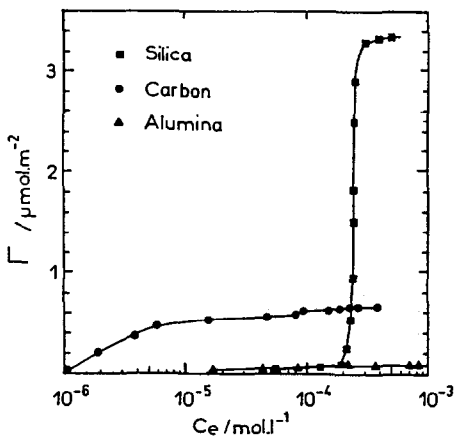

Fig. 3. Adsorption Isotherms of TX 100.

For silica : the adsorption isotherm is sigmoidal. Γ is 0.04 $\mu mol.m^{-2}$ when C_e= 5.10^{-5}-2.10^{-4} $mol.l^{-1}$, increases abruptly at C_e=$2.5.10^{-4}$ $mol.l^{-1}$ and reaches a plateau

corresponding to Γ_{max}=3.3 µmol.m^{-2} at C_e=4.4.10^{-4} mol.l^{-1}. This is slightly higher than the C.M.C (2.8.10^{-4} mol.l^{-1}).

For activated carbon : the isotherm starts at a very low equilibrium concentration C_e=10^{-6} mol.l^{-1}. At C_e=6.10^{-6} mol.l^{-1}, Γ is 0.5 µ mol.m^{-2}. For C_e values between 6.10^{-6} mol.l^{-1} and the C.M.C , Γ increases slightly and the Γ_{max}= 0.65 µmol.m^{-2} is reached at C_e=10^{-5}mol.l^{-1}.

For alumina : the adsorbed amount does not rise above 0.1µmol.m^{-2}.

B) OBS (Fig.4).

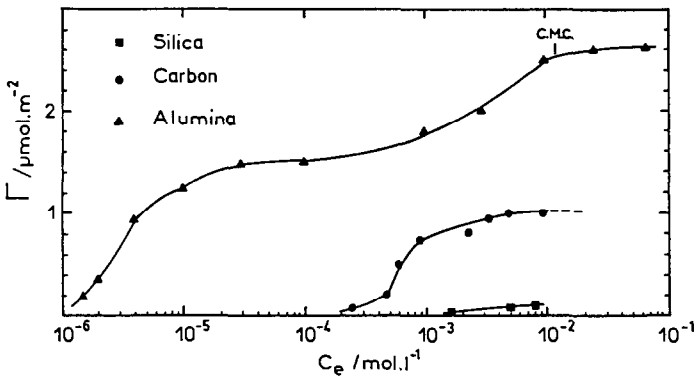

Fig. 4. Adsorption Isotherms of OBS.

For silica : virtually no adsorption takes place (Γ=0.02 µmol.m^{-2}).

For activated carbon : the isotherm starts at C_e = 2.10^{-4} mol.l^{-1} and reaches a plateau (1 µmol.m^{-2}) for C_e 5.10^{-3} mol.l^{-1}, much lower than the C.M.C (1.2.10^{-2} mol.l^{-1}).

For alumina : adsorption takes place for very low concentrations (10^{-6} mol.l^{-1}). Γ increases sharply to a first plateau at Γ=1.6 µmol.m^{-2} for C_e ranging from 2.10^{-5} to 2.10^{-4} mol.l^{-1}. For higher C_e values, Γ increases again and reaches the C.M.C. plateau with Γ max= 2.6µmol.m^{-2}

C) salicylate (Fig.5).

For silica : the adsorption is negligible.

For activated carbon : Γ increases regularly from C_e=5.10^{-4} mol.l^{-1} and reaches a pseudo-plateau (Γ_{max}=0,8 µmol.m^{-2}) for C_e > 10^{-2} mol.l^{-1}.

For alumina : the shape of the isotherm is similar to that for activated carbon. Γ increases regularly from C_e=4.10^{-6} mol.l^{-1} to a a pseudo-plateau (Γ_{max}=1.5 µmol.m^{-2}) at C_e > 1. 10^{-3} mol.l^{-1}.

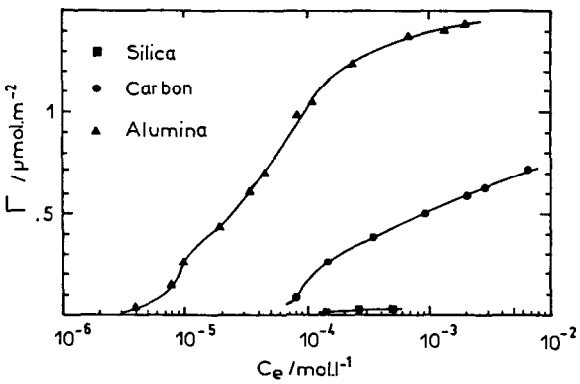

Fig. 5. Adsorption Isotherms of Salicylate.

Microcalorimetry

Figures 6 to 8 represent $\Delta_{dis}h$ in function of Γ for the adsorption of TX100 on the silica, of OBS and salicylate on the alumina, and of the three adsorbates on the activated carbon.

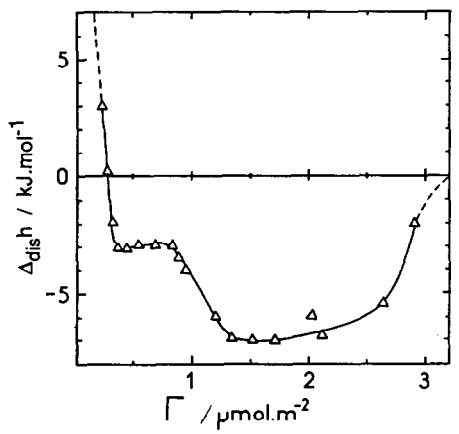

Fig. 6. Displacement Enthalpy versus TX 100 Adsorbed on Silica.

For silica (Fig.6), an exothermic signal is observed for adsorbed quantities lower than 0,3 µmol.m^{-2}. It becomes endothermic for the rest of the isotherm. This endothermic part exhibits a plateau at $\Delta_{dis}h$=3 kJ.mol^{-1} for Γ=0,3-0,8 µmol.m^{-2}, and a second plateau at

$\Delta_{dis}h$ =7 kJ.mol^{-1} for Γ=1,3-2,6 µmol.m^{-2}. The enthalpy is reduced to 0 when Γ reaches 3 µmol.m^{-2}.

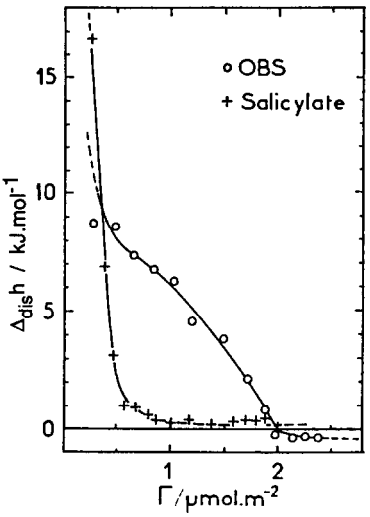

Fig. 7. Displacement Enthalpy versus OBS and Salicylate Adsorbed on Alumina.

For alumina (Fig.7) the adsorption of OBS and salicylate yields an exothermic signal. In the case of the salicylate, $\Delta_{dis}h$ ranges from -16,6 to 0 kJ.mol^{-1} when Γ rises from 0 to 1,4 µmol.m^{-2}, and remains close to 0 at higher values. For OBS $\Delta_{dis}h$ ranges from-8,5 to 0 kJ.mol^{-1} when Γ rises from 0 to 2 µmol.m^{-2} and then remains close to 0.

For activated carbon (Fig.8) the signals are exothermic and the enthalpies decrease regularly all along the isotherms. Their values start from -150 kJ.mol^{-1} for TX 100, 90 kJ.mol^{-1} for OBS and-80 kJ.mol^{-1} for salicylate, and are reduced to 0 at high values.

DISCUSSION

The adsorption isotherm of TX 100 on silica reveals a low adsorbate-adsorbent interaction: it covers a short scale of equilibrium concentrations (5.10^{-5} to the CMC : 4.10^{-4} mol.l^{-1}). The adsorption mechanisms have been clarified for this particular case (21) by means of fluorescence decay: for Γ lower than 0,3 µmol.m^{-2} only isolated molecules are adsorbed; for values ranging from 0,3 to 0,5 µmol.m^{-2} small micelle-like aggregates (less then 200 molecules) appear on the surface; for greater Γ values the clusters become infinite (19-22).

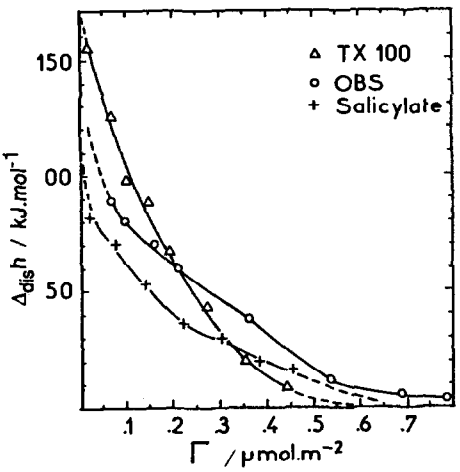

Fig. 8. Displacement Enthalpy versus TX 100, OBS and Salicylate Adsorbed on Activated Carbon.

The enthalpic curve (Fig.6) clearly confirms these mechanisms: the exothermic part fo the signal indicates the adsorption of the isolated TX 100 molecules; the endothermic part is typical of the micellization of this non-ionic surfactant (12). In the latter part the first plateau corresponds to the formation of the small clusters, the second as well as the evolution towards $\Delta_{dis}h = 0$, fits the formation of the large clusters. The normal adsorbate-adsorbent interaction could be a hydrogen bond between the predominating $\equiv SO^-$ sites (pH = 6 to 6.5, fig.1) and the oxyethylenic groups of the adsorbate.

On the alumina surface, which is positive at experimental pH (pH = 4,5 to 7,5:, fig 1), only a very low adsorption of TX 100 is observed (Fig.3). Yet the anionic molecules are adsorbed in large quantities (Fig.4 and 5). The prevailing normal adsorbate-adsorbent bond is an electrostatic interaction between the $\equiv AlOH_2^+$ sites and the $-COO^-$ and $-SO_3^-$ groups of the anionic adsorbates (23-25). It can also be observed that the OBS isotherm is located at lower C_e values than the salicylate isotherm. This originates from two factors. First, the affinity of the sulfonate group for the alumina sites is greater than that of the carboxylate group (26, 27). Conversely, the adsorbed phase is in a liquid crystal structure originating from the attractive interactions between the alkyl chains of the ionic surfactant molecules (28). The exothermic character of the enthalpic curves reflects both the strong affinity of the adsorbate for the alumina and the structurization of the adsorbed phase. Structurization yields an exothermic signal when it occurs in solution in form of the micellization (29).

On the activated carbon (Fig.8), the calorimetric signals are exothermic all along the isotherm. The enthalpy values are higher than in the case of silica and alumina and reach 80 to 150 $kJ.mol^{-1}$. By contrast with the alumina and silica surfaces, the activated carbone surface is hydrophobic and provokes only a weak structurization of the water molecules (30, 31). The work needed to displace those water molecules is therefore lower and the measured raw enthalpy approximates a true adsorption enthalpy. The adsorption mechanisms previously described cannot be proposed for such a surface: only the most hydrophobic parts of the adsorbates are in contact with it. The similarity between the three enthalpic curves suggests that the benzene ring, common to the three molecules participates in the adsorption because of its structural affinity with the graphitic layers of the activated carbon, implying short-distance Van der Waals' interactions (32). The alkyl chain is also in interaction with the surface of the solid, insofar as its presence in both surfactants entails higher enthalpies than those produced by the salicylate. In this case, by comparison with the silica, TX 100 is adsorbed either as isolated molecules, or in the form of aggregates, whose structure is different from the micelles, insofar as the plateau of the adsorption isotherm is reached for equilibrium concentrations much lower than the CMC.

CONCLUSION

Microcalorimetry can to measure the relative enthalpies of displacment of the structured water by adsorbate molecules on solid surfaces. When correlated to the study of the adsorption isotherms, it allows different mechanisms and changes in the structure of the adsorbed phase to be shown.

In the case of a weak adsorbate-adsorbent interaction (TX 100 adsorbed on the silica), microcalorimetry shows that micelles form on the solid surface at equilibrium concentrations near the CMC, and that they are of two types according to the coverage (micellar-sized aggregates, then large clusters). In a strong interaction system between anionic adsorbates and an electropositive surface (OBS and salicylate adsorbed on alumina), it shows that the mechanisms differ according to the nature of the adsorbates: in the case of OBS, the lateral interaction between the alkyl chains of the molecules in the adsorbed phase is added to the calorimetric signal due to the normal interaction.

On a hydrophilic solid (metallic oxides) the raw enthalpy values are decreased by the heat of displacement of the structured water. On a hydrophobic system such as activated carbon, weak structurization of the water molecules yields high raw enthalpy values, approximating to a real adsorption enthalpy. On such a solid the adsorption mechanisms are of two types: interaction between the hydrophobic part of the adsorbates (alkyl chains) and the solid, and interaction between the benzene ring and the graphitic layers.

REFERENCES

1 K.G. BARNETT, T. COSGROVE, B. VINCENT, D.S. SISSONS, M.A. COHEN-STUAT.

Macromolecules. 14 (1981) 10.
2 M. BRUANT, J.Y. BOTTERO, J.M. CASES, D. CANET, F. FIESSINGER. J. Colloid and Int. Sci.
(1987) submitted for publication.
3 P. VAN CUTSEM, C. GILLET, M.M. MESTDAGH, P.G. ROUXHET. In "interactions solide-liquide dans les milieux poreux" . J.M. CASES ed. Editions TECHNIP, Paris (1985) 171.
4 R. VAROQUI. Nouveau Jounal de Chimie. 6 (1982) 187.
5 M.A. COHEN-STUART, W.H. WAAJEN, S.S. DUKHIN. Colloid and Polym. Sci. 262 (1984) 423.
6 E. KILLMANN, R. ECKART. Makromol. Chem. 144 (1971) 45.
7 E. KILLMANN, K. WINTER. Angew. Makromoml. Chem. 35 (1975) 39.
8 E. KILLMANN, J. EISENLAUER, M. KORN. J. Polym. Sci. Polym. Symp. 61 (1977) 423.
9 S. PARTYKA, F. ROUQUEROL, J. ROUQUEROL. J. Colloid Int. Sci. 68 (1979) 21.
10 J. ROUQUEROL, S. PARTYKA. J. chem. Techn. and Biotechn. 31 (1981) 584.
11 J.C. NEGRE, R. DENOYEL, F. ROUQUEROL, J. ROUQUEROL. In "Interactions solide-liquide dans les milieux poreux". J. M. CASES Ed. Editions TECHNIP, Paris (1985) 463.
12 E. KEH, S. ZAINI, S. PARTYKA. J.C.A.T. Montpellier (1985) 463.
13 L. A. NOLL, T. E. BURCHFIELD. Colloids and Surfaces. 5 (1982) 33.
14 G. W. WOODBURY, L. A. NOLL. Colloids and Surfaces. 8 (1983) 1.
15 L. A. NOLL, G. W WOODBURY, T. E. BURCHFIELD. Colloids and Surfaces. 9 (1984) 349.
16 R. DENOYEL, F. ROUQUEROL, J. ROUQUEROL. In "Adsorption from Solution". R. H. OTTEWILL, C. H. ROCHESTER and A. L. SMITH Ed. Academic press. London (1983) 225.
17 J. ROUQUEROL. Internal Report. G. S. "Traitement Chimique des Eaux" (1985).
18 F. THOMAS. Internal Report. G. S. "Traitement Chimique des Eaux". (1984).
19 S. PARTYKA, M. LINDHEIMER, S. ZAINI, E. KEH, B. BRUN. In "Interactions solide-liquide dans les milieux poreux". J.M. CASES Ed. Editions TECHNIP, Paris (1985) 509.
20 J. J.FRIPIAT, J. M. CASES, M. FRANCOIS, M. LETELLIER. J. Colloid Int. Sci. 89 (1982) 378.
21 P. LEVITZ, H. VAN DAMME, H. KERAVIS. J. Phys. Chem. 88, 11 (1984) 2228.
22 J. M. CASES, P. LEVITZ, J. E. POIRIER, H. VAN DAMME. In "Advances in Mineral Processing" P. SOMASUNDARAN Ed. S.M.E. Pub. Littleton (1986) 171.
23 P. SOMASUNDARAN, D.W. FUERSTENAU. J. Phys. Chem. 70 (1966) 90.
24 J. F. SCAMEHORN, R. S. SCHECHTER, W. H. WADE. J. Colloid Int. Sci. 83, 2 (1982) 463.
25 F. THOMAS, J. Y. BOTTERO, J. M. CASES. (1987) to be published.
26 E. RAKOTONARIVO, J.Y. BOTTERO, J.M. CASES, A. LEPRINCE. Colloids and Surfaces. (1984) 273.
27 E. RAKOTONARIVO, J.Y. BOTTERO, J.M. CASES, A. LEPRINCE. Colloids and Surfaces. (1985) 153.
28 J. M. CASES. Bull. de Minéralogie. 102 (1979) 684.
29 S. PARTYKA, M. LINDHEIMER, J. Y. BOTTERO, B. BRUN, P. SOMASUNDARAN, K. U. VISWANATAN. J.C.A.T. Montpellier (1985) 76.
30 A. C. ZETTLEMOYER. Ind. and Eng. Chemistry. 57, 2 (1965) 27.
31 H. F. STOEKLI, F. KREEHENBUEHL. Carbon. 19, 5 (1981) 353.
32 M. LAYARD, O. DUSARD, M. MAZET. J. de Chimie Physique. 82, 4 (1985) 415.